Smart hydrogels based on double responsive triblock terpolymers†

Stefan Reinicke,[a] Joachim Schmelz,[a] Alain Lapp,[b] Matthias Karg,[c] Thomas Hellweg[c] and Holger Schmalz*[a]

Received 13th January 2009, Accepted 19th March 2009
First published as an Advance Article on the web 22nd April 2009
DOI: 10.1039/b900539k

In this work a new kind of "smart" hydrogel is presented, which is composed of a poly(2-vinylpyridine)-*block*-poly(ethylene oxide)-*block*-poly(glycidyl methyl ether-*co*-ethyl glycidyl ether) (P2VP-*b*-PEO-*b*-P(GME-*co*-EGE)) triblock terpolymer. The thermo-sensitive poly(glycidyl methyl ether-*co*-ethyl glycidyl ether) block exhibits a cloud point which is easily adjustable by the comonomer ratio. Copolymerization of GME and EGE produces nearly statistical copolymers with a weak preferential incorporation of GME, exhibiting a sharp coil-to-globule transition with almost no hysteresis. The triblock terpolymers aggregate in aqueous solution triggered by both pH and temperature. At sufficiently high concentration this stimuli-responsive behaviour leads to a reversible gel formation with gel strengths and transition points tuneable by pH, temperature, concentration, and block lengths. At pH = 7, an unique gel–sol–gel transition accompanied with a strengthening of the gel is observed upon heating using rheology. Moreover, the structure of the low temperature gel phase is investigated by means of small-angle neutron scattering (SANS).

Introduction

"Smart" hydrogels are networks of water soluble polymers which form/disintegrate or swell/contract upon changes of external stimuli like solution pH, temperature, or ionic strength. Such hydrogels can be utilized in drug delivery applications, since they can release trapped drug molecules upon shrinkage or disintegration.[1–3] Other applications can be found as storage media, in actuating systems, sensors, microfluidic switches, and many more.[4–6]

In general, one can distinguish between two classes of "smart" gels.[7] Chemically crosslinked stimuli-responsive polymers constitute the first category.[8] The most intensively studied example is chemically crosslinked poly(N-isopropylacrylamide) (PNIPAAm), a thermo-sensitive polymer becoming hydrophobic at around 32 °C, and very often used in hydrogel applications.[9–12] Other thermo-sensitive polymers used to construct such hydrogels are for instance poly(alkyl vinyl ethers),[13,14] chemically modified polyglycidols,[15] or copolymers of 2-(2-methoxyethoxy)ethyl methacrylate with oligo(ethylene glycol) methacrylate (P(MEO_2MA-*co*-OEGMA)).[16] A typical monomer used for the synthesis of pH-sensitive hydrogels is methacrylic acid.[17] The second class of hydrogels comprises physically crosslinked hydrogels, which disintegrate reversibly upon changes of a certain external parameter. Such systems are typically composed of linear or star-shaped block copolymers with an ABA and $(BA)_x$ structure, respectively. The A-block is stimuli-responsive, *i.e.* becomes hydrophobic at a certain pH or temperature, and therefore forms the network junctions. Examples are poly(ethylene oxide)-*block*-poly(N-isopropylacrylamide) (PEO-*b*-PNIPAAm)[18] and PEO-*b*-P(MEO_2MA-*co*-OEGMA)[19] star block copolymers, poly(ε-caprolactone)-*block*-poly(ethylene oxide)-*block*-poly(ε-caprolactone) (PCL-*b*-PEO-*b*-PCL) triblock copolymers,[20] ABC triblock terpolymers composed of different poly(alkyl vinyl ether)s,[21] or—as examples of pH-sensitive hydrogels—ABA and $(BA)_x$ block copolymers where A is poly(diethyl aminoethyl methacrylate) (PDEAEMA) and B poly(glycerol monomethacrylate) (PGMA).[22] Gels with permanent physical crosslinks, *i.e.* where the outer blocks are hydrophobic and not stimuli-responsive, are for instance based on ABCBA pentablock terpolymers with poly(methyl methacrylate) (PMMA) outer blocks, B is poly(acrylic acid) (PAA) and C is poly(2-vinylpyridine) (P2VP).[23] In addition, ABA triblock or multiblock copolymers consisting of poly(*n*-butyl acrylate) (P*n*BA), polystyrene (PS), poly(*n*-butyl methacrylate) (P*n*BMA) and poly(dimethylaminoethyl methacrylate) (PDMAEMA) blocks were described.[24,25] Other systems, like the well known Pluronic™ block copolymers, form gels by a regular packing of micelles, mostly in a cubic phase (bcc, or fcc).[26,27]

All examples discussed so far are hydrogels which respond to only one external stimulus, temperature or pH. However, some applications may require an independent response to several factors.[28] A suitable monomer for creating pH- and temperature-responsive hydrogels is DMAEMA.[29–31] Since the number of dual responsive monomers is limited, a thermo-sensitive monomer is often copolymerized with a pH-sensitive monomer in order to obtain a double stimuli-responsive gel.[32–34] Another approach utilizes interpenetrating networks or blends of two different stimuli-sensitive polymers.[35] One example for a double stimuli-responsive gel based on a crosslinked block copolymer with blocks responding to different stimuli is a P(DMAEMA-*co*-HEMA)-*b*-PNIPAAm-*b*-P(DMAEMA-*co*-HEMA) (HEMA = hydroxyethyl methacrylate) triblock copolymer.[36] However, all

[a]*Makromolekulare Chemie II, Universität Bayreuth, D-95440 Bayreuth, Germany*
[b]*Laboratoire Léon Brillouin, CEA de Saclay, 99191 Gif sur Yvette, France*
[c]*Physikalische Chemie I, Universität Bayreuth, D-95440 Bayreuth, Germany*

† Electronic supplementary information (ESI) available: Detailed information on the determination of reactivity ratios for GME/EGE copolymerization, and turbidimetry for various P(GME-*co*-EGE) copolymers. See DOI: 10.1039/b900539k

these systems belong to the class of chemically crosslinked gels. Examples of double responsive physical gels are still limited. They are formed for instance by a poly(N,N-diethylacrylamide)-*block*-poly(acrylic acid)-*block*-poly(N,N-diethylacrylamide) (PDEAAm-*b*-PAA-*b*-PDEAAm) ABA triblock copolymer,[37] or an ABCBA pentablock terpolymer, where A is a pH-sensitive poly(sulfamethazine methacrylate) block, B is PCL, and C is PEO.[38] With few exceptions, these polymers were synthesized by free radical polymerization or by atom transfer radical polymerization (ATRP) with limited control with respect to block length and polydispersity. An interesting approach towards temperature- and redox-responsive physical hydrogels is based on the incorporation of redox-cleavable disulfide linkages at the midpoint of ABA triblock copolymers with thermo-sensitive end blocks, *e.g.* PNIPAAm.[39,40]

Our approach towards double stimuli-responsive (pH and temperature) hydrogels is based on an ABC triblock terpolymer (Scheme 1), where A is pH-sensitive poly(2-vinylpyridine) (P2VP), B water soluble poly(ethylene oxide) (PEO), and C a thermo-sensitive copolymer of glycidyl methyl ether and ethyl glycidyl ether (P(GME-*co*-EGE)). At pH < 5, the 2VP units are protonated rendering the P2VP block hydrophilic,[41,42] *i.e.* at low pH and room temperature, the polymer is molecularly dissolved. Increasing the pH above 5, the P2VP block becomes hydrophobic due to deprotonation. This should result in the formation of core–shell–corona (CSC) micelles with P2VP cores. An inverse micellar structure, with the thermo-sensitive P(GME-*co*-EGE) block forming the core, should be obtained at low pH and for temperatures above the cloud point of P(GME-*co*-EGE). In both cases, a hydrogel might already be formed by close packing of CSC micelles for sufficiently high concentrations, *i.e.* analogous to the behaviour of Pluronics™ block copolymers.[26,27] However, upon applying the respective stimulus (pH or temperature) to switch the responsive corona block [P2VP or P(GME-*co*-EGE)] of the CSC micelles insoluble, too, hydrogel formation should take place (Scheme 1). This process is driven by the open association of CSC micelles, with physical crosslinks formed by the now insoluble corona blocks. Thus, depending on concentration, *i.e.* whether the CSC micelles already formed a gel or not, a hydrogel will be formed or the pre-formed hydrogel will transform into a stronger gel upon applying both stimuli. The produced hydrogel can be destroyed reversibly by adjusting either pH or temperature, resulting in a solubilization of the A or C block, respectively.

We use our recently developed synthetic route to produce P2VP-*b*-PEO-*b*-P(GME-*co*-EGE) triblock terpolymers in a one-pot reaction by sequential anionic polymerization of the corresponding monomers in THF.[43]

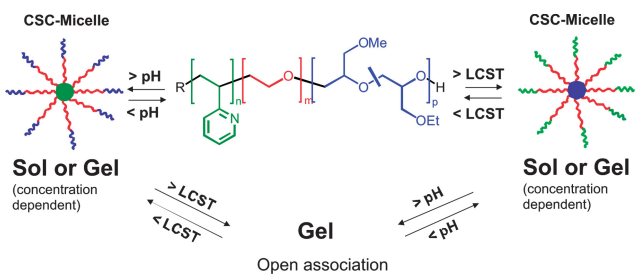

Scheme 1 Scheme of the formation of double responsive hydrogels based on P2VP-*b*-PEO-*b*-P(GME-*co*-EGE) triblock terpolymers.

The lower critical solution temperature (LCST) of alkyl glycidyl ethers is strongly affected by the length and structure of the alkyl chain.[44,45] The copolymerization of GME and EGE promised a way of adjusting the LCST over a wide temperature range simply by changing the copolymer composition, similar to the copolymerization of 2-(2-methoxyethoxy)ethyl methacrylate with oligo(ethylene glycol) methacrylate,[46] and of 2-*n*-propyl-2-oxazoline with 2-ethyl-2-oxazoline or 2-isopropyl-2-oxazoline.[47] Thus, prior to the triblock terpolymer synthesis the reactivity ratios for GME/EGE copolymerization were determined, and the dependence of the LCST-type phase separation of the resulting copolymers on the composition and concentration was investigated.

The results and discussion part will be divided into two subsections. First, we present the results of the GME/EGE copolymerization and the dependence of P(GME-*co*-EGE) cloud points on composition. The second part will deal with the synthesis and characterization of P2VP-*b*-PEO-*b*-P(GME-*co*-EGE) triblock terpolymers. The ability to form micellar aggregates in aqueous solution triggered by pH and temperature is demonstrated using dynamic light scattering. The pH and temperature dependent hydrogel formation and disintegration was monitored by the test tube inversion method as well as by rheology. At pH = 7, an unusual gel–sol–gel transition was observed upon heating, which goes along with a strengthening of the hydrogel. The influence of concentration and block lengths on the gel strength and the transition points was investigated, too. Finally, small-angle neutron scattering data are presented, which reveal the structure of the hydrogel in the low temperature regime.

Experimental

Materials

Tetrahydrofuran (Merck, p.a.) was purified by successive distillation over CaH_2 and potassium, and kept under dry nitrogen before use. Glycidyl methyl ether (TCI, >85%) was distilled with a Vigreux column, first, at atmospheric pressure and then at 100 mbar from powdered CaH_2, followed by a purification over *t*-BuOK in order to remove residual epichlorohydrin. Finally, GME was condensed into a glass ampoule for storage. Prior to use, it was purified over *n*-BuLi and condensed into a sampling ampoule. Ethyl glycidyl ether (TCI, >98%) was purified in the same way but without the distillation steps. Decane, used as internal standard for GC measurements, was purified over *n*-BuLi and condensed into a storage ampoule. The phosphazene base *t*-BuP_4 (Fluka, 1 M in hexane), *sec*-BuLi (Acros, 1.3 M in cyclohexane/hexane: 92/8), *n*-BuLi (Aldrich, 2 M in cyclohexane), *t*-BuOK (Aldrich, 1 M in THF) and *t*-BuOLi (Aldrich, 1 M in hexanes) were used as received. The *t*-BuOLi solution contained a small amount of *t*-BuOH, as detected by GC. 2-Vinylpyridine (Fluka, ≥97%) and ethylene oxide (Linde, 3.0) were purified as reported elsewhere.[43]

Polymerizations

Polymerizations were carried out in a thermostated laboratory autoclave (Büchi) under dry nitrogen atmosphere. The synthesis

of the GME/EGE copolymers was accomplished in THF by anionic ring-opening polymerization of the corresponding monomers using *t*-BuOK or *t*-BuOLi/*t*-BuP_4 as the initiator. In a typical procedure, the monomer mixture (17.9 mL) and decane (4 mL) were added to THF (200 mL) at 50 °C, followed by fast addition of the initiator. Samples were taken for conversion determination *via* gas chromatography (GC). After 2 days the reaction was terminated by adding a few mL of MeOH containing 1–2 droplets of conc. HCl. The copolymers with a low GME content were purified by evaporation of the solvent, followed by repeated dispersion in water and centrifugation at 40 °C. Copolymers with higher GME content were purified *via* dialysis against Millipore water using a cellulose ester dialysis tube with a MWCO of 500 g/mol (Spectra/Por™). After drying for 2–3 days under vacuum at 40 °C, the copolymers were obtained as highly viscous colourless or pale yellow liquids. The synthesis of the P2VP-*b*-PEO-*b*-P(GME-*co*-EGE) triblock terpolymers *via* sequential anionic polymerization and the subsequent purification was performed analogously to the recently reported procedure.[43]

Size exclusion chromatography (SEC)

SEC experiments were performed on an instrument equipped with four PSS SDV gel columns (porosities: 10^2, 10^3, 10^4 and 10^5 Å, diameter: 5 μm), a pre-column (10^2 Å, 5 μm), a differential refractometer (Shodex), and a UV-detector at 254 nm (Waters). A calibration with narrowly distributed polystyrene standards was used. Measurements were performed in THF at 40 °C with a flow rate of 1 mL/min using toluene as the internal standard.

Matrix assisted laser desorption ionization time of flight mass spectrometry (MALDI-ToF MS)

MALDI-ToF MS was performed on a Bruker Reflex III with a UV laser operating at 337 nm and an acceleration voltage of 20 kV. 1,8,9-Trihydroxyanthracene (dithranol) as matrix and silver triflate as cationizing agent were used for P2VP homopolymers. Samples were dissolved in THF (10 mg/mL) and mixed with matrix (20 mg/mL in THF) and salt (10 mg/mL in THF) at a mixing ratio of 20:5:1 (v/v, matrix: analyte: salt). 1 μL of this mixture was spotted onto the target and allowed to dry. 200–500 laser shots were accumulated for each spectrum.

Nuclear magnetic resonance spectroscopy (NMR)

The absolute number averaged molecular weight (M_n) of the synthesized triblock terpolymers was determined by ^{1}H-NMR in $CDCl_3$ (Bruker AC 250 spectrometer) using the absolute M_n of the P2VP block, determined by MALDI-ToF, for calibration of the NMR signal intensities.

Cloud point determination

The P(GME-*co*-EGE) copolymers were dissolved in Millipore water and the concentration was fixed at 2.5 g/L. The cloud points were determined by turbidity measurements using a titrator (Titrando 809, Metrohm, Herisau, Switzerland) equipped with a turbidity probe (λ_0 = 523 nm, Spectrosense, Metrohm) and a temperature sensor (Pt 1000, Metrohm). The temperature program (1 K/min) was run by a thermostat (LAUDA RE 306 and Wintherm_Plus software), using a home-made thermostatable vessel. The cloud points were determined from the intersection of the two tangents applied to the two linear regimes of the transmission curve at the onset of turbidity.

Sample preparation for micellisation and gelation experiments

The triblock terpolymers were dissolved in Millipore water or deionized water containing 0.1M NaCl. The pH was fixed at a value of 3–4 using conc. HCl (Riedel-de-Haën). Samples to be characterized under neutral conditions were then titrated slowly to pH = 7 (titer 1M NaOH, Titrisol, Merck; 0.13–0.67 μL/min). The titrations and pH-measurements were performed using a titrator (Titrando 809, Metrohm, Herisau, Switzerland), equipped with a titration unit (Dosino 800, Metrohm, Herisau, Switzerland) and a common glass membrane pH-electrode (micro electrode, Metrohm, Herisau, Switzerland).

Dynamic light scattering (DLS)

DLS was performed on an ALV DLS/SLS-SP 5022F compact goniometer system with an ALV 5000/E cross-correlator and a He-Ne laser (λ_0 = 632.8 nm). The solutions were filtered prior to the measurement with 0.8 μm syringe filters (Cameo). For temperature dependent measurements, the decaline bath of the instrument was thermostated using a LAUDA Proline RP 845 thermostat. The temperature was increased stepwise (2 K/step). After each step the sample was equilibrated for 10 min before data acquisition. pH dependent measurements were conducted using the DLS device in combination with a titrator (Titrando 809, Metrohm, Herisau, Switzerland). NaOH (titer 1M, Titrisol, Merck) was added in small portions of 2 μL. The equilibration time after each titration step was 3 min. The scattering intensity data presented correspond to an average of five measurements, conducted for 1 min each.

Test tube inversion

The glass tubes (volume 5 mL) containing the samples were immersed in an oil bath, which was heated stepwise (1 K/min) using a heating plate (RCT basic, IKA) equipped with a contact thermometer (Ikatron, IKA). After each temperature step the test tubes were inverted in order to check whether the sample flowed or not.

Rheology

For dynamic–mechanical measurements a Physica MCR 301 rheometer with a cone–plate shear cell geometry (d = 50 mm, cone angle = 1°) was used. Prior to the measurements the linear viscoelastic regime for each sample was determined by performing a strain sweep test at a frequency of 1 Hz. For all temperature dependent measurements a frequency of 1 Hz, a strain of 0.7%, and a heating rate of 0.1 K/min were applied. The temperature was controlled by a Peltier element. For frequency sweeps (10^{-1} to 10^2 Hz) at different temperatures the desired temperatures were adjusted by heating the sample slowly at a rate of 0.1 K/min.

Small-angle neutron scattering (SANS)

SANS experiments were performed using the PAXY instrument of the Laboratoire Léon Brillouin (CEA de Saclay). The scattered neutrons were collected employing a two-dimensional multi-detector. Three sample-to-detector distances of 1.05 m, 3.05 m, and 6.75 m were chosen to cover a rather large q-range. The sample temperature was controlled using a thermostat and a PT 100 temperature sensor leading to a stability of at least around ±0.5 °C. The samples were prepared in pure D_2O in order to guarantee high scattering contrasts and were measured in 1 mm standard quartz cells (Hellma, Germany).

Due to the isotropic character of the scattering patterns, the collected data were circularly averaged. The resulting spectra were then corrected for electronic noise, detector efficiency, and the scattering of the empty cell and the solvent. Normalisation to achieve absolute intensity values was done using the method developed by Cotton. Further information on the data treatment procedure of the LLB can be found elsewhere.[48,49] The data collected at the different sample-to-detector distances overlapped within the experimental precision after the treatment procedure. Hence, no further adjustment was necessary.

The normalised and merged scattering profiles were analyzed applying the SASfit program by Kohlbrecher.[50] The presented fits were done considering adjustable prefactors for the contrast of the different blocks. The model, which was chosen for the fitting process, comprises three different form factor contributions:

1. The form factor for a spherical core:

$$K(q, R, \Delta\eta) = \frac{4}{3}\pi R^3 \Delta\eta 3 \frac{(\sin(qR) - qR\cos(qR))}{(qR)^3}$$

Here, R is the core radius and Δη the scattering contrast.

2. The form factor for a spherical shell:

$$F(q,\ R,\ \nu R,\ \mu,\ \Delta\eta) = K(q,\ R,\ \Delta\eta) - K(q,\ \nu R,\ \Delta\eta)(1 - \mu)$$

Here, R is the outer radius, the fraction νR accounts for the core radius, μΔη defines the scattering contrast of the core and Δη is the scattering contrast of the shell.

3. The form factor for Gaussian polymer chains:

$$F^2(q, R_g, I_0) = I_0 2\left(\frac{(qR_g)^2 - 1 + \exp\left(-(qR_g)^2\right)}{(qR_g)^4}\right)$$

Here, R_g is the radius of gyration of the Gaussian polymer chains.

Further details on the SANS data analysis will be treated in the near future in a forthcoming work.

Results and discussion

Copolymerization of GME and EGE: reactivity ratios

The anionic ring-opening copolymerization of GME and EGE was carried out in THF at 50 °C using *t*-BuOK as the initiator. The conversions as well as the copolymer compositions were determined by gas chromatography (see ESI†). Identical conditions were applied for the *t*-BuOLi/*t*-BuP_4 initiating system, which was used as a model for the active chain end in the triblock terpolymer synthesis with respect to the polymerization of the glycidyl ether block.[43] The obtained P(GME-*co*-EGE) copolymers had a molecular weight of about 5000 g/mol with polydispersity indices PDI ≈ 1.07 (Table S1, ESI†).

The Skeist approach allows the determination of reactivity ratios from a single copolymerization experiment, as it considers the change in the feed composition when the reaction proceeds (integral copolymerization equation).[51] Thus, reactivity ratios can be calculated from higher conversions, too, in contrast to the well known Fineman–Ross procedure.[52] The solution of the integral copolymerization equation published by Meyer *et al.*[53,54] was used to calculate the reactivity ratios numerically. In addition, the Fineman–Ross method was used for copolymerizations with *t*-BuOK. A detailed description concerning the determination of reactivity ratios is provided in the ESI.†

The reactivity ratios obtained from the Skeist approach for *t*-BuOK as the initiator are r(GME) = 1.42 and r(EGE) = 0.53, respectively, *i.e.* there is only a week preferential incorporation of GME into the propagating chain (Table S2, ESI†). Consequently, we obtained nearly statistical copolymers showing a very weak gradient in composition along the chain. The reactivity ratios determined by the Fineman–Ross method are r(GME) = 1.31 and r(EGE) = 0.55 (Fig. S1, ESI†), which is in good agreement with the values obtained from the Skeist approach, showing its applicability. Finally, comparing these values with the ones obtained from the copolymerization with *t*-BuOLi/*t*-BuP_4, r(GME) = 1.33 and r(EGE) = 0.72, reveals that the initiating system does not influence the copolymerization behaviour significantly.

Synthesis of P2VP-*b*-PEO-*b*-P(GME-*co*-EGE)

The general strategy for the synthesis of the P2VP-*b*-PEO-*b*-P(GME-*co*-EGE) triblock terpolymers was already described in detail in a previous publication.[43] All three blocks were synthesized within one step by sequential monomer addition. First, 2-vinylpyridine was polymerized followed by ethylene oxide. Since the chain end of the "living" polymer carries a lithium counter ion, it is necessary to add the phosphazene base *t*-BuP_4 after the addition of ethylene oxide, which promotes ethylene oxide polymerization.[55–57] Finally, an equimolar GME/EGE mixture was added. For molar ratios of GME/EGE to initiator higher than 80, we observed transfer reactions to the glycidyl ether monomers,[58] limiting the maximum achievable P(GME-*co*-EGE)

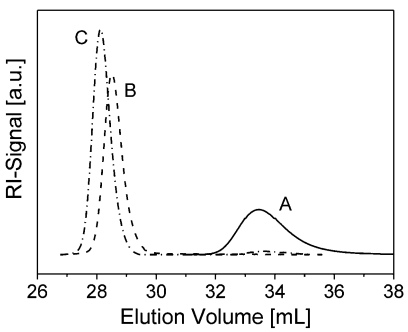

Fig. 1 THF-SEC traces of a $P2VP_{57}$-*b*-PEO_{477}-*b*-P(GME_{22}-*co*-EGE_{22}) triblock terpolymer before purification (C) and its corresponding P2VP (A) and P2VP-*b*-PEO (B) precursors.

Table 1 Molecular characteristics of P2VP-*b*-PEO-*b*-P(GME-*co*-EGE) triblock terpolymers

Sample	DP[a] (P2VP)	DP[b] (PEO)	DP[b] (GME-*co*-EGE)	M_n (10^{-3} g/mol)[b]/M_w/M_n[c]
1	57	477	22–22	31.2/1.02
2	62	452	36–36	33.2/1.02
3	33	236	11–12	16.0/1.02

[a] Determined *via* MALDI-ToF. [b] Determined from ^{1}H-NMR spectra using the absolute M_n(P2VP) for signal intensity calibration. [c] Determined *via* THF-SEC with polystyrene calibration.

block length. However, the produced P(GME-*co*-EGE) homopolymer can be easily removed from the triblock terpolymer by precipitation in diethyl ether. SEC analysis (Fig. 1) shows, that P2VP-*b*-PEO-*b*-P(GME-*co*-EGE) triblock terpolymers with narrow molecular weight distributions were obtained (PDI $\approx$ 1.02), and polymerization proceeds without significant side reactions when keeping the molar ratio of glycidyl ether monomers to initiator below 80.

The molecular characteristics of the synthesized triblock terpolymers are summarized in Table 1.

Thermoresponsiveness of GME/EGE copolymers

For the investigation of the temperature dependent solubility of the GME/EGE copolymers five different comonomer ratios were chosen (see Table S1, ESI†). Aqueous solutions with a concentration of 2.5 g/L were prepared, and the temperature dependent transmittance was measured at a heating rate of 1 K/min (Fig. S2, ESI†).

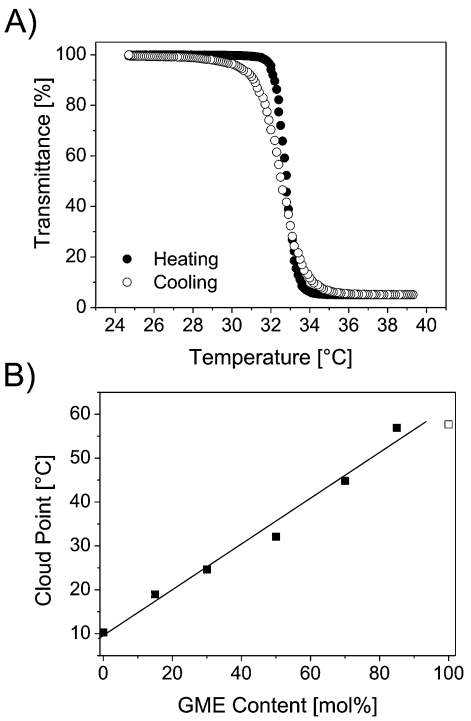

Fig. 2 (A) Transmittance curves (heating–cooling cycle) for an aqueous solution of P(GME-*co*-EGE) with 50 mol% GME (2.5 g/L, 1 K/min), and (B) cloud points of P(GME-*co*-EGE) copolymers and their dependence on the GME content (heating rate 1 K/min, 2.5 g/L in water, quality factor of the linear fit: 0.99); the open square corresponds to the cloud point of a homo-PGME taken from literature.[45]

A representative heating–cooling cycle for a P(GME-*co*-EGE) with 50 mol% GME is shown in Fig. 2A. The coil-to-globule transition of the copolymer is still very sharp, irrespective of the small compositional gradient along the chain. Similar observations were reported by Park and Kataoka for gradient copolymers of 2-*n*-propyl-2-oxazoline and 2-isopropyl-2-oxazoline.[47] Furthermore, the cloud point of the P(GME-*co*-EGE) copolymers depends linearly on the copolymer composition (Fig. 2B), which was observed for 2-alkyl-2-oxazoline gradient copolymers, too. Most interestingly, the P(GME-*co*-EGE) copolymers show almost no hysteresis within one heating–cooling cycle (Fig. 2A), similar to the poly(oligo(ethylene glycol) methacrylate) copolymers prepared by Lutz *et al.*[46]

Aggregation of P2VP-*b*-PEO-*b*-P(GME-*co*-EGE)

According to Scheme 1 we expect that the P2VP-*b*-PEO-*b*-P(GME-*co*-EGE) triblock terpolymers form core–shell–corona micelles under conditions where only one of the two outer blocks is insoluble, *i.e.* at room temperature and high pH, or at elevated temperatures and low pH. This was verified by light scattering measurements, recording the scattering intensities of diluted aqueous solutions of $P2VP_{62}$-*b*-PEO_{452}-*b*-P(GME_{36}-*co*-EGE_{36}) as a function of pH and temperature.

Fig. 3A shows the count rate of a 1 g/L aqueous solution of $P2VP_{62}$-*b*-PEO_{452}-*b*-P(GME_{36}-*co*-EGE_{36}) versus pH. At low pH a very small count rate is observed, which is due to the fact that only unimers are present under these conditions. Upon reaching a pH value of around 5, the count rate increases significantly and reaches a plateau for pH > 5.5. The transition is very sharp, and the corresponding pH value coincides very well with values already published.[41,42] At this point the P2VP block becomes insoluble, resulting in the formation of core–shell–corona micelles with a P2VP core (Scheme 1). What is not shown here but nevertheless is worth to be mentioned is that the micelle formation is fully reversible.

Fig. 3B presents the count rate of the same solution and its dependence on the temperature at pH = 3, *i.e.* the P2VP block is protonated and therefore soluble. To avoid interactions between the charged P2VP blocks the measurements were performed in the presence of salt (0.1M NaCl). At room temperature the count rate is very low and starts to increase strongly at 45 °C, *i.e.* the polymer chains start to aggregate at that point. The transition is not as sharp as in the case of the pH dependent measurement, the count rate continues to increase up to temperatures of 65 °C. Ogura *et al.* showed for PEO-*b*-PEGE diblock copolymers with a comparable temperature-sensitive PEGE block, that at

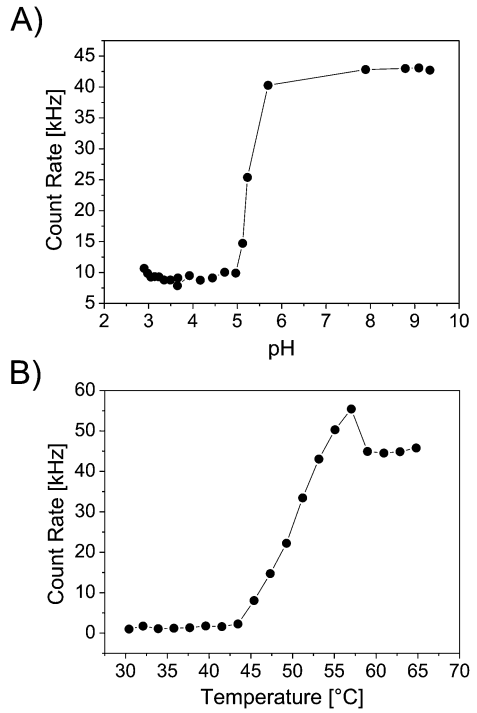

Fig. 3 Scattering intensity at $\theta = 90°$ of a 1 g/L solution of $P2VP_{62}$-*b*-PEO_{452}-*b*-P(GME_{36}-*co*-EGE_{36}) plotted vs. (A) pH at room temperature (titer 1M NaOH, stepwise addition of 2 μL, equilibration time 3 min), and (B) temperature at pH = 3 (0.1M NaCl, 2 K/step, equilibration time 10 min).

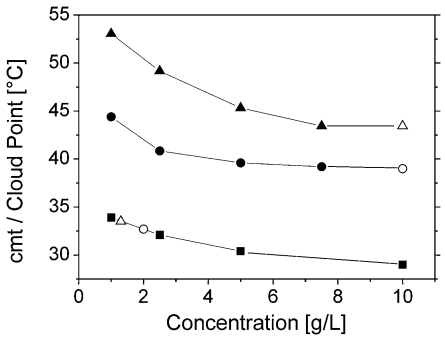

Fig. 4 Critical micellisation temperatures (cmt)/cloud points of different P2VP-*b*-PEO-*b*-P(GME-*co*-EGE) triblock terpolymers (at pH = 3, 0.1M NaCl) and a P(GME-*co*-EGE) homopolymer as a function of concentration: $P2VP_{57}$-*b*-PEO_{477}-*b*-P(GME_{22}-*co*-EGE_{22}) (▲); $P2VP_{62}$-*b*-PEO_{452}-*b*-P(GME_{36}-*co*-EGE_{36}) (●); P(GME-*co*-EGE), 50 mol% GME, M_n = 5,000 g/mol (■); the open symbols represent samples having the same concentration with respect to the P(GME-*co*-EGE) block, highlighting the shift to higher temperatures caused by the hydrophilic PEO and P2VP blocks.

temperatures above 40 °C PEO already starts to lose some of the bound water in its hydration shell, but still being well soluble. This results in a further increase in the hydrodynamic radius of the micelles despite the fact that the core forming PEGE block (cloud point of *ca.* 10 °C) is already strongly hydrophobic in this temperature range.[59] Partial dehydration of PEO at temperatures above 40 °C was observed for other PEO containing block copolymers, too.[60–62] Thus, the observed temperature induced aggregation over a broad temperature range is not only caused by the coil-to-globule transition of the P(GME-*co*-EGE) block, but is presumably combined with the start of dehydration of the PEO, too.

Fig. 4 shows the critical micellisation temperatures (cmt's), which correspond to the onset of the count rate increase upon heating (Fig. 3B), of two triblock terpolymers and their dependence on concentration. Compared to the cloud points of the P(GME-*co*-EGE) homopolymer (50 mol% GME) a significant shift of the cmt to higher temperatures can be observed. For $P2VP_{57}$-*b*-PEO_{477}-*b*-P(GME_{22}-*co*-EGE_{22}) the difference is 10 °C and for $P2VP_{62}$-*b*-PEO_{452}-*b*-P(GME_{36}-*co*-EGE_{36}) 6.4 °C, respectively, for identical concentrations with regard to the thermo-sensitive P(GME-*co*-EGE) block (see open symbols in Fig. 4). This result marks the influence of the attached hydrophilic PEO and P2VP (protonated at pH = 3) blocks, a common phenomenon already described in the literature.[63] As a conclusion, the P(GME-*co*-EGE) block should have a minimum block length in order to maintain its switchability at moderate temperatures, as the cmt increases with decreasing block length. Furthermore, the cmts/cloud points decrease with increasing concentration and level off at concentrations of about 8–10 g/L. This is in contrast to the results reported by Watanabe and coworkers, revealing a less pronounced concentration dependence of the cloud point of a PEGE homopolymer.[59] A detailed investigation of the aggregation behaviour of the P2VP-*b*-PEO-*b*-P(GME-*co*-EGE) triblock terpolymers is in progress and will be the topic of a forthcoming publication.

Gel formation and rheology

As already discussed in the Introduction, aqueous solutions of P2VP-*b*-PEO-*b*-P(GME-*co*-EGE) triblock terpolymers are supposed to form hydrogels under conditions where both end blocks are insoluble, *i.e.* at high pH and temperature (Scheme 1). Alternatively, hydrogels might be formed by close packing of core–shell–corona micelles, too. In this case, only one of the end blocks is insoluble, *i.e.* at high pH and low temperature (only P2VP insoluble), or at low pH and high temperature (only P(GME-*co*-EGE) insoluble). Hence, the ability of the synthesized P2VP-*b*-PEO-*b*-P(GME-*co*-EGE) triblock terpolymers to form hydrogels, and the respective response of the hydrogels to pH/temperature was studied in detail.

In order to investigate the gelation behaviour of our triblock terpolymers, we prepared aqueous solutions with concentrations between 10 and 18 wt% at pH = 3 followed by a slow titration to pH = 7 (titer 1M NaOH, 0.13–0.67 μL/min). At pH = 7 solutions of $P2VP_{57}$-*b*-PEO_{477}-*b*-P(GME_{22}-*co*-EGE_{22}) and $P2VP_{62}$-*b*-PEO_{452}-*b*-P(GME_{36}-*co*-EGE_{36}) form free standing gels already at room temperature at concentrations ≥14 wt% and ≥12 wt%, respectively, as revealed by the test tube inversion method (Fig. 5A). The hydrogels are typically slightly turbid with a bluish colour, which might indicate a certain inhomogeneity of the samples.

In order to verify the thermoresponsiveness, the hydrogel based on $P2VP_{57}$-*b*-PEO_{477}-*b*-P(GME_{22}-*co*-EGE_{22}) (18 wt%, pH = 7) was heated from 20 °C to 65 °C, and the presence of a gel state was verified by the test tube inversion method (Fig. 5A–C).

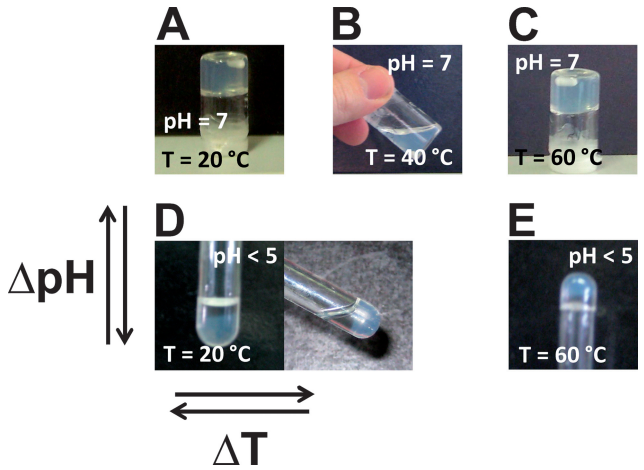

Fig. 5 Photographs of an 18 wt% solution of $P2VP_{57}$-*b*-PEO_{477}-*b*-$P(GME_{22}$-*co*-$EGE_{22})$ at different pH and temperatures.

The first observation is a "melting" of the hydrogel at temperatures between 25–35 °C, resulting in a viscous liquid. However, at temperatures between 40 and 45 °C, which coincide very well with the observed cmt (Fig. 4), the gel state is restored due to the thermo-sensitive P(GME-*co*-EGE) block becoming hydrophobic at that point, and thus forming the network junctions. A similar behaviour was observed for $P2VP_{62}$-*b*-PEO_{452}-*b*-$P(GME_{36}$-*co*-$EGE_{36})$, with a slight shift of the corresponding transition temperatures to lower values, due to the increased P(GME-*co*-EGE) block length. This kind of gel–sol–gel transition upon heating is rather unusual, and is mostly accompanied by a softening of the gel at higher temperatures.[62,64,65]

The hydrogel formed by $P2VP_{57}$-*b*-PEO_{477}-*b*-$P(GME_{22}$-*co*-$EGE_{22})$ at pH = 7 and room temperature can be disintegrated by the addition of HCl (solubilization of P2VP), which produces a clear solution being able to flow again. Most interestingly, the gel can be simply restored at elevated temperatures (Fig. 5D and E). This is observed for $P2VP_{62}$-*b*-PEO_{452}-*b*-$P(GME_{36}$-*co*-$EGE_{36})$, too. It is noted, that a $P2VP_{33}$-*b*-PEO_{236}-*b*-$P(GME_{11}$-*co*-$EGE_{12})$ triblock terpolymer, with identical composition compared to $P2VP_{57}$-*b*-PEO_{477}-*b*-$P(GME_{22}$-*co*-$EGE_{22})$ but only half the overall molar mass does not form a gel at any temperature or pH up to concentrations of 30 wt%. Thus, a minimum molar mass is required to obtain a gel at reasonable concentrations.

The thermo-responsive behaviour of our gels was investigated more systematically by rheology. We applied an oscillatory stress to the sample using a cone-plate shear cell geometry. Regimes with $G' > G''$ are referred to as gel state with respect to the common definitions.[66]

In Fig. 6A, the storage (G') and loss (G'') modulus are plotted vs. the temperature for an 18 wt% solution of $P2VP_{57}$-*b*-PEO_{477}-*b*-$P(GME_{22}$-*co*-$EGE_{22})$. Between 20 and 35 °C G' exceeds G'' significantly, *i.e.* the solution is in the gel state. At 35 °C G' crosses G'', thus, at that point we reach the sol state with G' being significantly lower compared to G''. Finally, G' exceeds G'' again at temperatures >48 °C, *i.e.* the gel state is restored. These results agree well with the observations made by the test tube inversion method (Fig. 5A–C). The value of G' at 60 °C is significantly higher compared to that at 20 °C. Hence, the gel–sol–gel

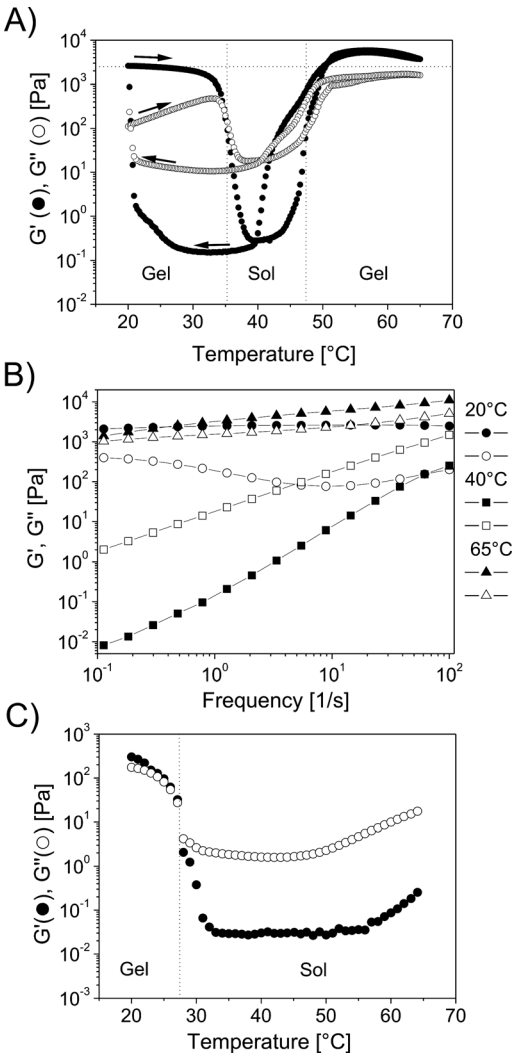

Fig. 6 Rheological properties of aqueous $P2VP_{57}$-*b*-PEO_{477}-*b*-$P(GME_{22}$-*co*-$EGE_{22})$ solutions (0.7% strain): (A) temperature dependent G' and G'' of an 18 wt% solution at pH = 7 (0.1 K/min), (B) frequency dependent G' (filled symbols) and G'' (open symbols) of an 18 wt% solution at pH = 7 for different temperatures, and (C) temperature dependent G' and G'' of a 13 wt% solution at pH = 7 (0.1 K/min).

transition upon heating is accompanied by a strengthening of the hydrogel. This behaviour is quite unique, as usually a softening of the gel is observed for comparable transitions.[62,64,65] The whole process is fully reversible, however, the reformation of the low temperature gel phase is significantly shifted to lower temperatures. This might be due to the mechanical stress which is applied to the solution during the measurement. Mechanical stress hinders the reformation of the micellar structures building the gel (see discussion of SANS experiments).

Another proof for the presence of a gel is a weak linear dependence/independence of G' on frequency. For $G' \propto \omega^2$ and $G'' \propto \omega^1$ we deal with a viscoelastic fluid. In this case G' is always lower than G''. Fig. 6B shows the frequency dependence of G' and G'' at different temperatures. At 20 °C G' is nearly constant in the range 10^{-1}–10^2 Hz, and G'' shows a broad minimum. This is characteristic for gels formed by cubic micellar phases,[67–70] and is supported by our SANS experiments, which will be discussed

later. At 40 °C G′ and G″ both increase with increasing frequency, with $G' \propto \omega^{1.7}$ and $G'' \propto \omega^{1}$, which is characteristic for the sol state. In the high temperature gel state at 65 °C, G′ exceeds G″ again and both moduli run almost parallel with frequency, showing a weak linear dependence on frequency. The dynamic behaviour of crosslinked chemical and physical gels at the gel point is given by the relation $G' \propto G'' \propto \omega^{n}$, *i.e.* G′ and G″ are parallel in a log–log plot.[66,71,72] This supports the proposed crosslinking of CSC micelles with a P2VP core by the thermo-sensitive P(GME-*co*-EGE) corona block above the cmt, resulting in a reformation of the gel *via* open association (Scheme 1).

A 13 wt% solution of $P2VP_{57}$-*b*-PEO_{477}-*b*-P(GME_{22}-*co*-EGE_{22}) undergoes only a gel–sol transition upon heating (Fig. 6C). Although the viscosity starts to increase significantly at around 45 °C the gel state is not reached anymore. A further decrease in concentration leads to a solution which is in the sol state over the whole measured temperature range. After screening a series of concentrations we can conclude that a gel–sol transition occurs for $P2VP_{57}$-*b*-PEO_{477}-*b*-P(GME_{22}-*co*-EGE_{22}) only between 12 and 16 wt%. At slightly higher concentrations, *i.e.* 18 wt%, a gel–sol–gel transition is observed upon heating.

Switching to $P2VP_{62}$-*b*-PEO_{452}-*b*-P(GME_{36}-*co*-EGE_{36}), *i.e.* increasing only the block length of the thermo-sensitive block from 44 to 72 repeating units, while keeping the concentration at 18 wt%, the behaviour does not change qualitatively (Fig. 7A). However, the high temperature gel state is restored at about 10 °C lower compared to $P2VP_{57}$-*b*-PEO_{477}-*b*-P(GME_{22}-*co*-EGE_{22}), which is in line with the observed lowering of the cmt with increasing block length of the P(GME-*co*-EGE) block (Fig. 4). In addition, the storage modulus increases from 5.4 kPa at 20 °C to 11.5 kPa at 60 °C, indicating a strengthening of the gel at higher temperatures. Finally, G′ and G″ of an 18 wt% solution of $P2VP_{62}$-*b*-PEO_{452}-*b*-P(GME_{36}-*co*-EGE_{36}) were monitored at pH = 3.5 as a function of temperature, too (Fig. 7B). In that case, a sol–gel transition occurs at about 46 °C, which was also observed for $P2VP_{57}$-*b*-PEO_{477}-*b*-P(GME_{22}-*co*-EGE_{22}). These results are in good agreement with the observations made by the test tube inversion method (Fig. 5D and E).

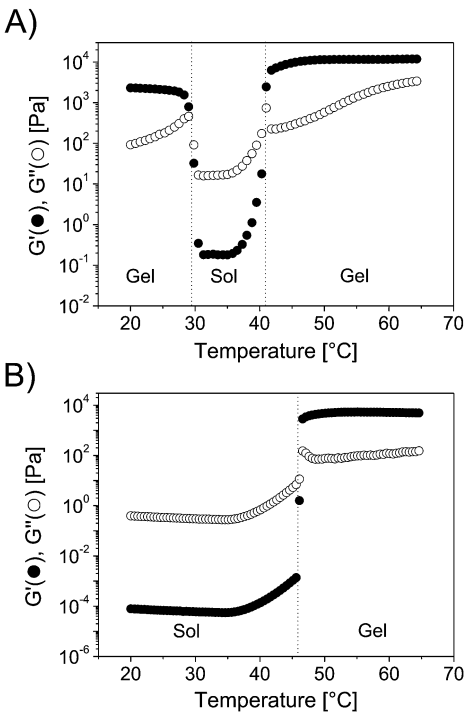

Fig. 7 Temperature dependent G′ and G″ for an 18 wt% solution of $P2VP_{62}$-*b*-PEO_{452}-*b*-P(GME_{36}-*co*-EGE_{36}): (A) at pH = 7, and (B) at pH = 3.5 (0.1 K/min, strain = 1%).

Small-angle neutron scattering

In order to gain a better understanding of the internal structure of the hydrogels at room temperature and pH = 7, we have performed SANS experiments on $P2VP_{62}$-*b*-PEO_{452}-*b*-P(GME_{36}-*co*-EGE_{36}) in D_2O at different concentrations.

Scattering of the 1.2 wt% solution is mostly determined by the form factor of the triblock terpolymer micelles (Fig. 8). The data can be well described with a core–shell model with additional Gaussian chains accounting for the soft corona. Fig. 8 compares the measured SANS profile and the respective fit, which was done using the SASfit program by Kohlbrecher.[50] The insoluble P2VP forms the core, while the highly swollen shell and corona are formed by the soluble PEO and P(GME-*co*-EGE) blocks, respectively. The fit gives a core radius of 6.5 nm for the triblock terpolymer micelles. The total radius including the shell is found to be 12.6 nm. In addition, a Guinier radius of the coiled chains in the micellar corona of 2.0 nm is computed. These values are in rather good agreement with the block length of the investigated triblock terpolymer (Table 1). Using the hydrodynamic radius of the block copolymer micelles obtained by DLS, a ratio ρ of approximately 0.45 is obtained.[73] This is significantly below the hard sphere value and in good agreement with a strongly swollen corona.

Scattering profiles for different concentrations are shown in Fig. 9. Already at a concentration of 2.4 wt% interactions between the micelles become important, which is reflected by the appearance of a structure factor maximum at $q \approx 0.012$ Å^{-1}. This maximum shifts to higher q-values with increasing concentration and gets more pronounced, *i.e.* the distance between the micelles decreases and the micellar assembly exhibits increased order.

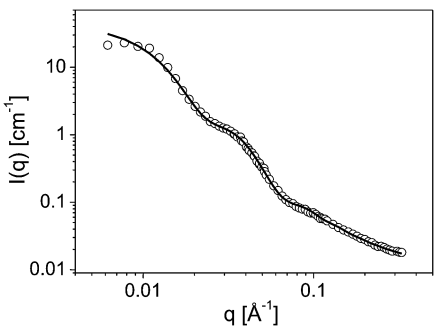

Fig. 8 SANS data for a 1.2 wt% solution of $P2VP_{62}$-*b*-PEO_{452}-*b*-P(GME_{36}-*co*-EGE_{36}) in D_2O at 20 °C and pH = 7. The solid line is a fit with a core–shell model plus Gaussian chains. The fit was done using the SASfit program by Kohlbrecher.[50]

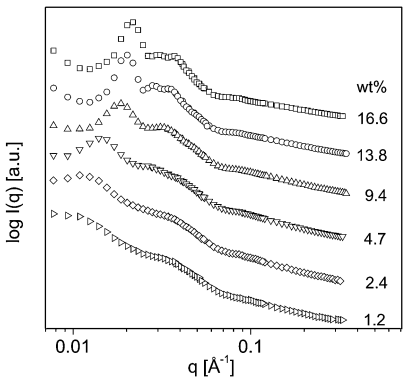

Fig. 9 SANS data for P2VP$_{62}$-*b*-PEO$_{452}$-*b*-P(GME$_{36}$-*co*-EGE$_{36}$) solutions in D_2O at 20 °C and pH = 7. The curves were shifted vertically for clarity.

In the SANS profile of the 16.6 wt% solution clearly 2 well-defined higher order reflections are visible, corresponding to relative peak positions of $1:2^{1/2}:3^{1/2}$ (Fig. 10). This is consistent with a simple cubic (sc) or body centred cubic (bcc) packing of the spherical CSC micelles. Due to a lack of higher order reflexes an assignment to sc or bcc is not possible. However, a bcc-type packing of spherical micelles is frequently observed for comparable diblock copolymer micelles having a star-like architecture, *i.e.* the soluble corona forming block is significantly larger compared to the insoluble core forming block, which supports a bcc-type structure for our system, too.[74–76] We plan to perform SANS experiments under shear in order to differentiate between a sc- and bcc-type packing. This method was used to determine the exact structure of the micellar packing in aqueous solutions of star block copolymers composed of PEO and PPO, *i.e.* bcc-type packing, which was not possible by SANS under static conditions.[77]

At this point we are not able to provide a detailed mechanism for the observed gel–sol–gel transition upon heating. In order to investigate the underlying structural changes, extensive SANS experiments are necessary and will be performed in the near future. However, based on our results a tentative mechanism might be given. At room temperature and pH = 7 the gel is formed by a cubic packing of spherical CSC micelles (probably bcc structure), as shown by SANS. Upon increasing temperature, but still below the cmt of the triblock terpolymers at low pH (Fig. 4), the P(GME-*co*-EGE) blocks start to lose some bound water, similar to PEO but at significantly lower temperatures.[41,59–62] This induces a shrinkage of the micelles, which will result in the observed transition into a sol phase if the volume fraction of micelles is below the critical value for a bcc phase ($\Phi = 0.68$). A further increase in temperature above the cmt of the triblock terpolymers will make the outer P(GME-*co*-EGE) blocks insoluble, thus reforming the gel by additional physical crosslinking of the CSC micelles. The presence of additional network points is supported by the higher storage modulus of the gel phase at elevated temperatures compared to that at room temperature, and by the corresponding change in the frequency dependence of G′ and G″, too (Fig. 6, 7).

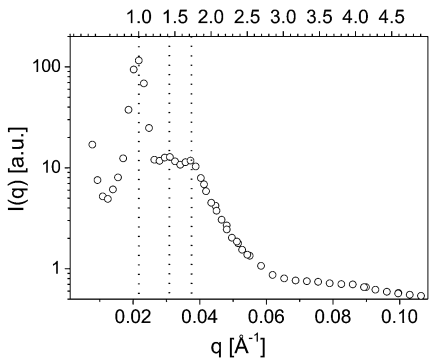

Fig. 10 SANS data for a 16.6 wt% solution of P2VP$_{62}$-*b*-PEO$_{452}$-*b*-P(GME$_{36}$-*co*-EGE$_{36}$) in D_2O, top x-axis normalized to 1st order reflection.

Conclusions

We successfully synthesized well-defined double stimuli-responsive P2VP-*b*-PEO-*b*-P(GME-*co*-EGE) triblock terpolymers by means of sequential anionic polymerization. The thermo-sensitive outer block consists of a glycidyl methyl ether (GME)/ethyl glycidyl ether (EGE) copolymer. Even though the copolymers exhibit a small compositional gradient, the coil-to-globule transition remains sharp, and the cloud point is easily adjustable by the comonomer ratio. Since both outer blocks of the triblock terpolymer are stimuli-responsive, a micellisation of the triblock terpolymer in aqueous solution under conditions where at least one outer block is hydrophobic takes place, *i.e.* pH = 7 and room temperature, or pH = 3 and temperatures above 40 °C. At pH = 7 and sufficiently high concentrations a unique gel–sol–gel transition is observed upon heating, which is accompanied with a strengthening of the hydrogel. Depending on block lengths, concentration, and pH, one additionally observes gel–sol and sol–gel transitions, and the gel strengths as well as the gel–sol and sol–gel transition temperatures vary. The low temperature gel at pH = 7 is based on a cubic arrangement of spherical CSC micelles with P2VP cores, as was shown using SANS experiments.

Acknowledgements

We would like to thank Jérôme Crassous (PC I, University of Bayreuth) for the introduction into rheological measurements, and Alejandro Müller (Universidad Simón Bolívar) for helpful discussions. Financial support from the German Science Foundation (priority program SPP 1259) is gratefully acknowledged.

References

1 Y. Tachibana, M. Kurisawa, H. Uyama, T. Kakuchi and S. Kobayashi, *Chem. Lett.*, 2003, **32**, 374–375.
2 D. S. Hart and S. H. Gehrke, *J. Pharm. Sci.*, 2007, **96**, 484–516.
3 L. Yu and J. Ding, *Chem. Soc. Rev.*, 2008, **37**, 1473–1481.
4 D. J. Beebe, J. S. Moore, J. M. Bauer, Q. Yu, R. H. Liu, C. Devadoss and B.-H. Jo, *Nature*, 2000, **404**, 588–590.
5 P. Calvert, P. Patra and D. Duggal, *Proc. SPIE-Int. Soc. Opt. Eng.*, 2007, **6524**, 65240M/1–65240M/6.
6 M. Guenther, D. Kuckling, C. Corten, G. Gerlach, J. Sorber, G. Suchaneck and K.-F. Arndt, *Sens. Actuators B*, 2007, **126**, 97–106.
7 S.-k. Ahn, R. M. Kasi, S.-C. Kim, N. Sharma and Y. Zhou, *Soft Matter*, 2008, **4**, 1151–1157.

8 K. Dušek ed., *Responsive Gels: Volume Transitions I/II in Adv. Polym. Sci*, 1993, 109/110.
9 X.-Z. Zhang and R.-X. Zhuo, *Eur. Polym. J.*, 2000, **36**, 643–645.
10 D. Kuckling, C. D. Vo, H.-J. P. Adler, A. Völkel and H. Cölfen, *Macromolecules*, 2006, **39**, 1585–1591.
11 T. G. Park and A. S. Hoffman, *J. Polym. Sci., Part A: Polym. Chem.*, 1992, **30**, 505–507.
12 K. Kratz, T. Hellweg and W. Eimer, *Ber. Bunsen Ges.*, 1998, **102**, 1603–1608.
13 D. Theiss, T. Schmidt and K.-F. Arndt, *Macromol. Symp.*, 2004, **210**, 465–474.
14 R. Reichelt, T. Schmidt, D. Kuckling and K.-F. Arndt, *Macromol. Symp.*, 2004, **210**, 501–511.
15 A. Utrata-Wesolek, B. Trzebicka, A. Dworak, S. Ivanova and D. Christova, *e-Polymers*, 2007, 19.
16 J.-F. Lutz, K. Weichenhan, Ö. Akdemir and A. Hoth, *Macromolecules*, 2007, **40**, 2503–2508.
17 H. He, L. Li and L. J. Lee, *Polymer*, 2006, **47**, 1612–1619.
18 H. H. Lin and Y. L. Cheng, *Macromolecules*, 2001, **34**, 3710–3715.
19 N. Fechler, N. Badi, K. Schade, S. Pfeifer and J.-F. Lutz, *Macromolecules*, 2009, **42**, 33–36.
20 S. J. Bae, M. K. Joo, Y. Jeong, S. W. Kim, W. K. Lee, Y. S. Sohn and B. Jeong, *Macromolecules*, 2006, **39**, 4873–4879.
21 S. Sugihara, S. Kanaoka and S. Aoshima, *J. Polym. Sci., Part A: Polym. Chem.*, 2004, **42**, 2601–2611.
22 P. D. Iddon and S. P. Armes, *Eur. Polym. J.*, 2007, **43**, 1234–1244.
23 N. Stavrouli, I. Katsampas, S. Angelopoulos and C. Tsitsilianis, *Macromol. Rapid Commun.*, 2008, **29**, 130–135.
24 N. A. Hadjiantoniou and C. S. Patrickios, *Polymer*, 2007, **48**, 7041–7048.
25 M. Achilleos, T. Krasia-Christoforou and C. S. Patrickios, *Macromolecules*, 2007, **40**, 5575–5581.
26 G. Wanka, H. Hoffmann and W. Ulbricht, *Macromolecules*, 1994, **27**, 4145–4159.
27 P. Alexandridis and T. A. Hatton, *Colloids Surf. A: Physicochem. Eng. Aspects*, 1995, **96**, 1–46.
28 L.-C. Dong and A. S. Hoffman, *J. Controlled Release*, 1991, **15**, 141–152.
29 M.-H. Han, J.-W. Kim, J. Kim, J. Y. Ko, J. J. Magda and I. S. Han, *Polymer*, 2003, **44**, 4541–4546.
30 B. Yildiz, B. Isik, M. Kis and O. Birgül, *J. Appl. Polym. Sci.*, 2003, **88**, 2028–2031.
31 F. A. Plamper, M. Ruppel, A. Schmalz, O. Borisov, M. Ballauff and A. H. E. Müller, *Macromolecules*, 2007, **40**, 8361–8366.
32 X.-Z. Zhang, Y.-Y. Yang, F.-J. Wang and T.-S. Chung, *Langmuir*, 2002, **18**, 2013–2018.
33 M. Karg, I. Pastoriza-Santos, B. Rodriguez-González, R. von Klitzing, S. Wellert and T. Hellweg, *Langmuir*, 2008, **24**, 6300–6306.
34 K. Kratz, T. Hellweg and W. Eimer, *Colloids Surf. A: Physicochem. Eng. Aspects*, 2000, **170**, 137–149.
35 J. Shi, N. M. Alves and J. F. Mano, *Macromol. Biosci.*, 2006, **6**, 358–363.
36 F.-J. Xu, E.-T. Kang and K.-G. Neoh, *Biomaterials*, 2006, **27**, 2787–2797.
37 S. A. Angelopoulos and C. Tsitsilianis, *Macromol. Chem. Phys.*, 2006, **207**, 2188–2194.
38 K. Dayananda, B. S. Pi, B. S. Kim, T. G. Park and D. S. Lee, *Polymer*, 2007, **48**, 758–762.
39 C. Li, J. Madsen, S. P. Armes and A. L. Lewis, *Angew. Chem. Int. Ed.*, 2006, **45**, 3510–3513.
40 A. P. Vogt and B. S. Sumerlin, *Soft Matter*, 2009, DOI: 10.1039/b817586a, Advance Article.
41 M. Vamvakaki, L. Papoutsakis, V. Katsamanis, T. Afchoudia, P. G. Fragouli, H. Iatrou, N. Hadjichristidis, S. P. Armes, S. Sidorov, D. Zhirov, V. Zhirov, M. Kostylev, L. M. Bronstein and S. H. Anastasiadis, *Faraday Discuss.*, 2005, **128**, 129–147.
42 J. Yin, D. Dupin, J. Li, S. P. Armes and S. Liu, *Langmuir*, 2008, **24**, 9334–9340.
43 A. A. Toy, S. Reinicke, A. H. E. Müller and H. Schmalz, *Macromolecules*, 2007, **40**, 5241–5244.
44 A. Labbe, S. Carlotti, A. Deffieux and A. Hirao, *Macromol. Symp.*, 2007, **249/250**, 392–397.
45 S. Aoki, A. Koide, S.-I. Imabayashi and M. Watanabe, *Chem. Lett.*, 2002, 1128–1129.
46 J.-F. Lutz, Ö. Akdemir and A. Hoth, *J. Am. Chem. Soc.*, 2006, **128**, 13046–13047.
47 J. S. Park and K. Kataoka, *Macromolecules*, 2007, **40**, 3599–3609.
48 A. Brulet, D. Lairez, A. Lapp and J.-P. Cotton, *J. Appl. Crystallogr.*, 2007, **40**, 165–177.
49 J.-P. Cotton, in *Neutron, X-Ray and Light Scattering*, ed. P. Lindner and T. Zemb, Elsevier Science Publishers B.V., Amsterdam, The Netherlands, 1991.
50 J. Kohlbrecher, *SASfit: A Program for Fitting Simple Structural Models to Small Angle Scattering Data*, Paul Scherrer Institut, Laboratory for Neutron Scattering, CH-5232, Villigen Switzerland, 2008.
51 I. Skeist, *J. Am. Chem. Soc.*, 1946, **68**, 1781–1784.
52 M. Fineman and S. D. Ross, *J. Polym. Sci.*, 1950, **5**, 259–262.
53 V. E. Meyer and G. G. Lowry, *J. Polym. Sci., Part A: Polym. Chem.*, 1965, **3**, 2843–2851.
54 R. K. S. Chan and V. E. Meyer, *J. Polym. Sci. Polym. Symp.*, 1968, **25**, 11–21.
55 B. Esswein, A. Molenberg and M. Möller, *Macromol. Symp.*, 1996, **107**, 331–340.
56 B. Esswein and M. Möller, *Angew. Chem. Int. Ed.*, 1996, **35**, 623–625.
57 H. Schmalz, M. G. Lanzendörfer, V. Abetz and A. H. E. Müller, *Macromol. Chem. Phys.*, 2003, **204**, 1056–1071.
58 A. Stolarzewicz, *Makromol. Chem.*, 1986, **187**, 745–52.
59 M. Ogura, H. Tokuda, S.-I. Imabayashi and M. Watanabe, *Langmuir*, 2007, **23**, 9429–9434.
60 H. Li, G.-E. Yu, C. Price, C. Booth, E. Hecht and H. Hoffmann, *Macromolecules*, 1997, **30**, 1347–1354.
61 R. K. Prud'homme, G. Wu and D. K. Schneider, *Langmuir*, 1996, **12**, 4651–4659.
62 V. Castelletto, I. W. Hamley, R. J. English and W. Mingvanish, *Langmuir*, 2003, **19**, 3229–3235.
63 C. M. Schilli, M. Zhang, E. Rizzardo, S. H. Thang, Y. K. Chong, K. Edwards, G. Karlsson and A. H. E. Müller, *Macromolecules*, 2004, **37**, 7861–7866.
64 M. Almgren, W. Brown and S. Hvidt, *Colloid Polym. Sci.*, 1995, **273**, 2–15.
65 A. Kelarakis, V. Castelletto, C. Chaibundit, J. Fundin, V. Havredaki, I. W. Hamley and C. Booth, *Langmuir*, 2001, **17**, 4232–4239.
66 H. H. Winter and M. Mours, *Adv. Polym. Sci.*, 1997, **134**, 165–234.
67 S. Barbosa, M. A. Cheema, P. Taboada and V. Mosquera, *J. Phys. Chem. B*, 2007, **111**, 10920–10928.
68 I. W. Hamley, *Phil. Trans. R. Soc. Lond. A*, 2001, **359**, 1017–1044.
69 J. L. Jones and T. C. B. McLeish, *Langmuir*, 1995, **11**, 785–792.
70 M. B. Kossuth, D. C. Morse and F. S. Bates, *J. Rheol.*, 1999, **43**, 167–196.
71 F. Chambon and H. H. Winter, *J. Rheol.*, 1987, **31**, 683–697.
72 H. W. Richtering, K. D. Gagnon, R. W. Lenz, R. C. Fuller and H. H. Winter, *Macromolecules*, 1992, **25**, 2429–2433.
73 W. Burchard and W. Richtering, *Prog. Colloid Polym. Sci.*, 1989, **80**, 151–163.
74 A. P. Gast, *Langmuir*, 1996, **12**, 4060–4067.
75 I. W. Hamley, C. Daniel, W. Mingvanish, S.-M. Mai, C. Booth, L. Messe and A. J. Ryan, *Langmuir*, 2000, **16**, 2508–2514.
76 G. A. McConnell, A. P. Gast, J. S. Huang and S. D. Smith, *Phys. Rev. Lett.*, 1993, **71**, 2102–2105.
77 C. Perreur, J.-P. Habas, J. Francois, J. Peyrelasse and A. Lapp, *Phys. Rev. E*, 2002, **65**, 041802/1–041802/7.